JOURNAL OF MATERIALS SCIENCE 30 (1995) 3874–3882

Interfacial reaction and adhesion between SiC and thin sputtered cobalt films

C.S. LIM*
Department of Material Chemical Engineering, Chonnam National University, Kwangju 500-757, Korea

H. NICKEL, A. NAOUMIDIS, E. GYARMATI
Institute for Materials in Energy Systems, Research Center Jülich, D-52425 Jülich, Germany

Thin sputtered cobalt films on SiC were annealed in an Ar/4 vol% H_2 atmosphere at temperatures between 500 and 1450 °C for various times. The reaction process and the reaction-product morphology were characterized using optical microscopy, surface profilometry, X-ray diffraction, scanning electron microscopy and electron probe microanalysis. The relative adhesive strength between the film and substrate was determined by the scratch test method. Below 850 °C sputtered cobalt with a thickness of 2 μm on SiC showed no detectable reaction products. Cobalt initially reacted with SiC at 850 °C producing Co_2Si and unreacted cobalt in the reaction zone. At 1050 °C the first-formed Co_2Si layer reacted to CoSi, and carbon precipitates were formed in the reaction zones. Sputtered thin cobalt layers reacted completely with SiC after annealing at 1050 °C for 2 h. Above 1250°C only CoSi was observed with carbon precipitates having an oriented structure in the reaction zone. Above 1450°C, a significant amount of graphitic carbon in the reaction zone was detected.

1. Introduction

SiC is used for high-temperature applications such as turbines [1, 2] and possibly advanced aerospace applications [3] in the form of monolithic ceramic or in ceramic or metal-matrix composites due to its excellent corrosion and erosion resistance. SiC is also a useful semiconducting material for high-temperature, high-frequency and high-power electronic devices. The large band gap of 2.9 eV allows SiC to be used in a variety of solid state electronic devices such as blue-light emitting diodes (LED). The high electron mobility of $1000\ cm^2\ V^{-1}$ and high drift velocity of $2.5 \times 10^7\ cm\,s^{-1}$ in SiC exceed the corresponding values for silicon by more than a factor of 2. These properties and the high thermal stability allow high-power and high-frequency operation at elevated temperatures [4, 5].

In all these applications, as well as for the process of joining SiC to SiC and SiC to metal with metallic intermediates, detailed knowledge about SiC/metal interactions and the thermal stability of SiC/metal interfaces is of primary importance [6–8]. The chemical, thermal and crystallographic compatibility, which is dependent on the interfacial reaction, thermal expansion mismatch and lattice mismatch, must be considered to establish the minimal stress gradients across the formed reaction zone.

In the case of other more common semiconducting devices, knowledge of the reactivity, thermal stability, and electronic structure of semiconductor–metal interfaces is extremely important for understanding the devices and controlling device performances. As in the case of silicon–metal contacts, the interaction between the SiC and a metal during thermal annealing determines the properties of the contacts. One area of interest is the use of metals forming silicides on SiC substrates at low temperature, in the attempt to form contacts with thermal annealing. Many metals have a strong tendency to interdiffuse at semiconductor–metal interfaces and most metals readily form carbides or silicides. A thorough characterization and understanding of SiC–metal interfaces, in terms of reactivity and thermal stability, is therefore crucial in the design of SiC devices. At present only a few detailed studies of the interaction of SiC with various types of metals have been reported [9–12].

Cobalt was chosen for this study because it could be used to make good high-temperature contacts for utilizing the properties of SiC. It is also of specific interest due to its silicide-forming tendency at low temperature. In this paper, the formation of SiC/Co interfaces in the temperature range between 500 and 1450 °C was studied. The adhesion of the formed interface between the polycrystalline SiC and the thin cobalt layers is discussed on the basis of measurement of the critical load, using the scratch test. Furthermore, a thermodynamic consideration was made for interpreting the interactions in the SiC/Co system.

2. Experimental procedure

The starting materials used for the experiments were high-density sintered α-SiC from "Elektroschmelzwerk Kempten", ESK, and thin sputtered cobalt films. The polycrystalline SiC contained 1.5 wt % total impurities, such as carbon and aluminium as specified by the manufactor (ESK). The carbon and aluminium, used as a sintering aid, decrease the grain-boundary energy to change the relationship between grain-boundary energy and surface energy. SiC plates were cut into small pieces with a diameter of 20mm and a thickness of 3mm and ground with a BN/C disc. The ground SiC samples were ultrasonically cleaned in ethanol, rinsed with water and dried. After the grinding process, the surface of the samples showed an average roughness of 32.6nm (measured by surface profilometry). The SiC plates were then polished with a diamond disc using diamond pastes of 30, 15, 3, 1 μm and hyprez liquids (polishing solution). After polishing, the surface showed an average roughness of 4.7 nm. The polished SiC was etched with Murakami solution prepared from 3 g KOH and 30 g K_3 $[Fe(CN)_6]$ in 60 ml H_2O at boiling temperature for 13 min. The etched SiC surface in Fig. 1 shows a typical mixed structure of globular form to long/plate form, and the average grain size is about 4 μm.

A cobalt film was sputter-deposited on to the polished SiC substrates in a commercial sputter equipment (Leybold/Germany, type Z-400). A magnetron-type D.C. sputtering source was used to deposit the coatings. Flowing argon was employed as a sputter gas with a partial pressure of 4.0×10^{-2} mbar. D.C. potentials were varied between 400 and 500V depending on the current density and pressure. The temperature of the substrate during deposition was estimated to be between 50 and 250 °C. Film thicknesses were measured by the observation of film steps on reference substrates using surface profilometry. Prior to coating, the thickness of the cobalt films was controlled by covering the substrate holders and by exposing the substrates for predetermined times. The applied film thickness was fixed at 2.0 μm for this study. This thickness allows the penetration of the CuK_α beam entirely into the reaction zone for investigating the reaction products by X-ray diffraction analysis (XRD).

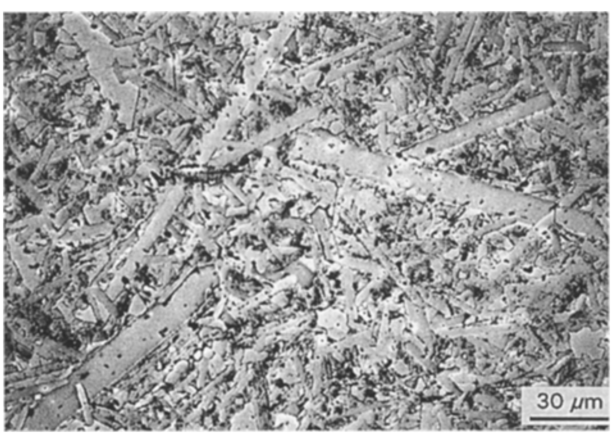

Figure 1 Scanning electron micrograph of the SiC surface etched for 13 min by a boiling Murakami solution of 3 g KOH and 30 g K_3 $(Fe(CN)_6$ in 60 ml H_2O).

Most systematic annealings were conducted in a high-temperature vacuum furnace with a graphite heating element manufactured by Degussa/Germany. SiC/Co samples were placed in a graphite crucible. The specimens were surrounded by titanium to remove the residual oxygen during the annealing time. After positioning the samples, the furnace was evacuated to 6×10^{-6} mbar and subsequently filled with a gas mixture of Ar/4 vol % H_2 for the annealing time. Thermocouples of type EL 18 (PtRh30/PtRh6) were used for temperature measurement in the range 500–1450 °C for 0.5–2 h. The heating rate was set between 20 and 30 K min^{-1} and the cooling rate between 5 and 10 K min^{-1}.

After reaction runs, the samples were characterized at the surface and in cross-section. The macroscopic variation of the surface structure and the progress of the reaction on the surface were examined by optical microscopy, scanning electron microscopy (SEM) and surface profilometry. The qualitative progress of the reaction in SiC/Co couples was estimated by determining phase fractions from relative XRD peak intensities of at least three coincidence-free reflections. The scratch test revealed the adhesive strength of the annealed samples by measurement of the critical load for film debonding. The reaction zone was analysed on a cross-section by optical microscopy, SEM and electron probe microanalysis (EPMA). For examination of cross-sections, all samples were cut by a diamond saw, coated with nickel by electrical deposition and then embedded in copper resin. After mounting, the reaction couples were ground on a diamond disc, and polished with diamond pastes of 30,15,6,3 and 1μm. The surface was finally polished with Al_2O_3 suspension.

3. Results

Fig. 2 shows the typical as-sputtered surface of cobalt film on a SiC substrate (SEM). The surface is composed of many solidified bubble shapes about 0.1–0.5μm diameter. According XRD analysis, the deposited cobalt film was crystallized hexagonally.

Fig.3 represents the measurements of the thickness of the sputtered cobalt as a function of the sputter times in the range from 0–7 h. The growth rate of cobalt films was calculated to be 11.7 nm/min^{-1} under the conditions used (magnetron sputter system, D.C. potential 500 V, partial pressure of Ar 4×10^{-2} mbar).

3.1. Surface morphology

Annealing experiments were performed in the temperature range between 500 and 1450 °C. In most cases, thin metal films were well coupled with the ceramic after annealing at temperatures between 850 and 1450 °C. A reaction product was initially detected at 850°C (after 4 h). Photographs of the surface of the reaction couples of SiC/Co after annealing at 650, 850, 1050 and 1450 °C are shown in Fig. 4. After annealing at 650 °C (Fig. 4a) no distinct changes on the surface

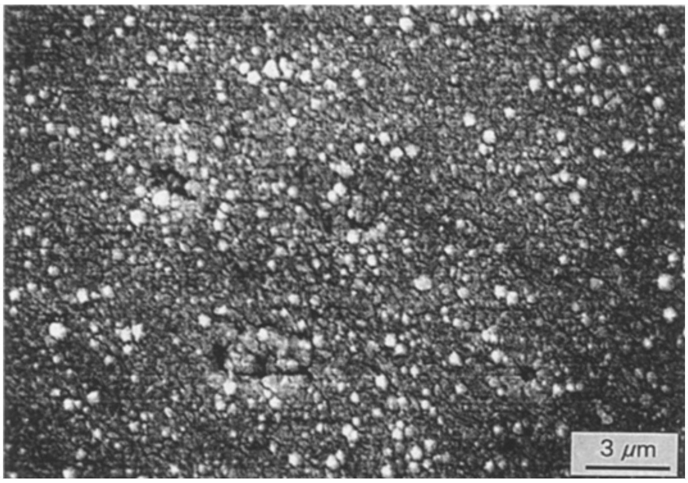

Figure 2 Scanning electron micrograph surface structure of the cobalt film (2 μm thick) deposited on the SiC substrate.

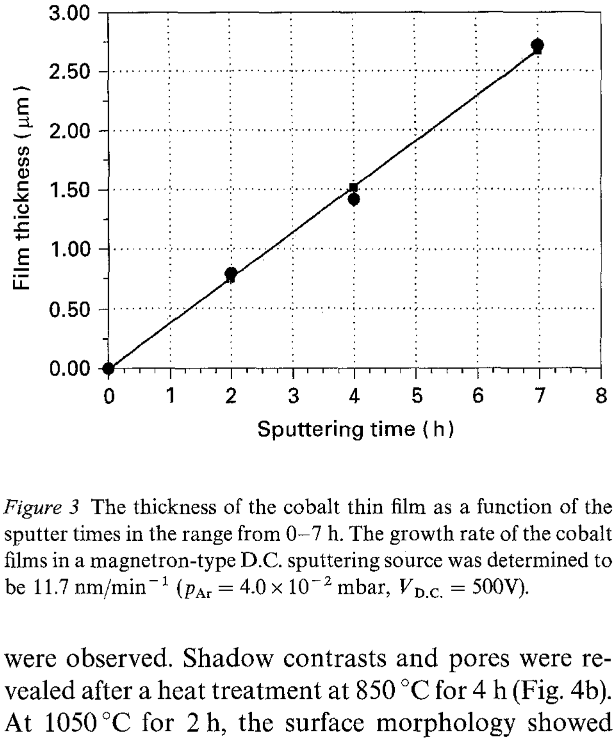

Figure 3 The thickness of the cobalt thin film as a function of the sputter times in the range from 0–7 h. The growth rate of the cobalt films in a magnetron-type D.C. sputtering source was determined to be 11.7 nm/min^{-1} ($p_{Ar} = 4.0 \times 10^{-2}$ mbar, $V_{D.C.} = 500V$).

were observed. Shadow contrasts and pores were revealed after a heat treatment at 850 °C for 4 h (Fig. 4b). At 1050 °C for 2 h, the surface morphology showed increased pore growth and crack formation (Fig. 4c). After annealing at 1450 °C, severe reactions were observed among the randomly distributed precipitations on the surface (Fig. 4d). On this sample, graphite formation was identified by XRD analysis. The extent of the reaction was indicated by the measurement of surface roughness with a surface profilometer. In Fig. 5, the average roughness of the annealed surface is shown after annealing at 650, 1050 and 1450 °C. The roughness of the surface was increased with increasing annealing temperature: 0.06, 0.26 and 1.67 μm, respectively.

3.2. Reaction products

The identification of reaction products was confirmed by determining the relative XRD peak intensities. Fig. 6 shows the qualitative phase analysis of the SiC/Co reaction couples based on the XRD analysis for different temperatures and times. Below 750 °C, no reaction was observed. At 850 °C, most of the cobalt-layer reacted and formed the silicide Co_2Si. Unreacted cobalt initially crystallized hexagonally, as identified by XRD, after this heat treatment as the cubic modification. It was distributed predominantly in the film surface. No carbide formation, either Co_2C or Co_3C, was detected by XRD.

At 1050 °C the entire cobalt film was consumed after 0.5 h. At this temperature, the amount of CoSi phase increased with annealing time by decreasing the fraction of Co_2Si phase. Co_2Si was fully consumed after 2 h (Fig. 7). The relative quantities of both silicides, estimated from XRD peak intensity ratios as a function of annealing time at 1050 °C, are listed in Table I. The same reaction stage was reached at 1250 °C after 0.5 h. After 2 h at 1250 °C small quantities of graphite could be detected, presumably developing by the graphitization of carbon formed through the reaction $Co + SiC \rightleftharpoons CoSi + C$. The quantity of graphite formed increased with the annealing temperature and time above 1250 °C. At 1450 °C, graphite was detected by XRD as the predominate reaction product and was epitaxially deposited on the surface of the sample. This confirms the optical observations reported in the previous section.

Cross-sectional views of annealed samples treated at 850 °C for 4 h were analysed by EPMA. Fig. 8 shows the line scan of the elemental cobalt, silicon and carbon across the reaction zone. The corresponding phase distribution is noted on this diagram. On the surface, a $Co + Co_2Si$ region was identified. In the areas adjacent to the SiC interface, a mixture of Co_2Si with carbon was formed.

A cross-sectional scanning electron micrograph (Fig. 9) shows the reaction zone after annealing at 1050 °C for 0.5 h. In the region neighbouring the SiC, a layer of CoSi was observed with randomly precipitated carbon. On the surface of this sample a layer was formed consisting of Co_2Si without carbon. The reaction zone between cobalt and SiC after an annealing at 1050 °C for 0.5 h can be described by the structure: $Co_2Si/CoSi/CoSi + C/CoSi/CoSi + C/ \dots /SiC$. Depending on the annealing time at this temperature, the relative quantities of CoSi increased simultaneously, while Co_2Si decreased. After 2 h at this

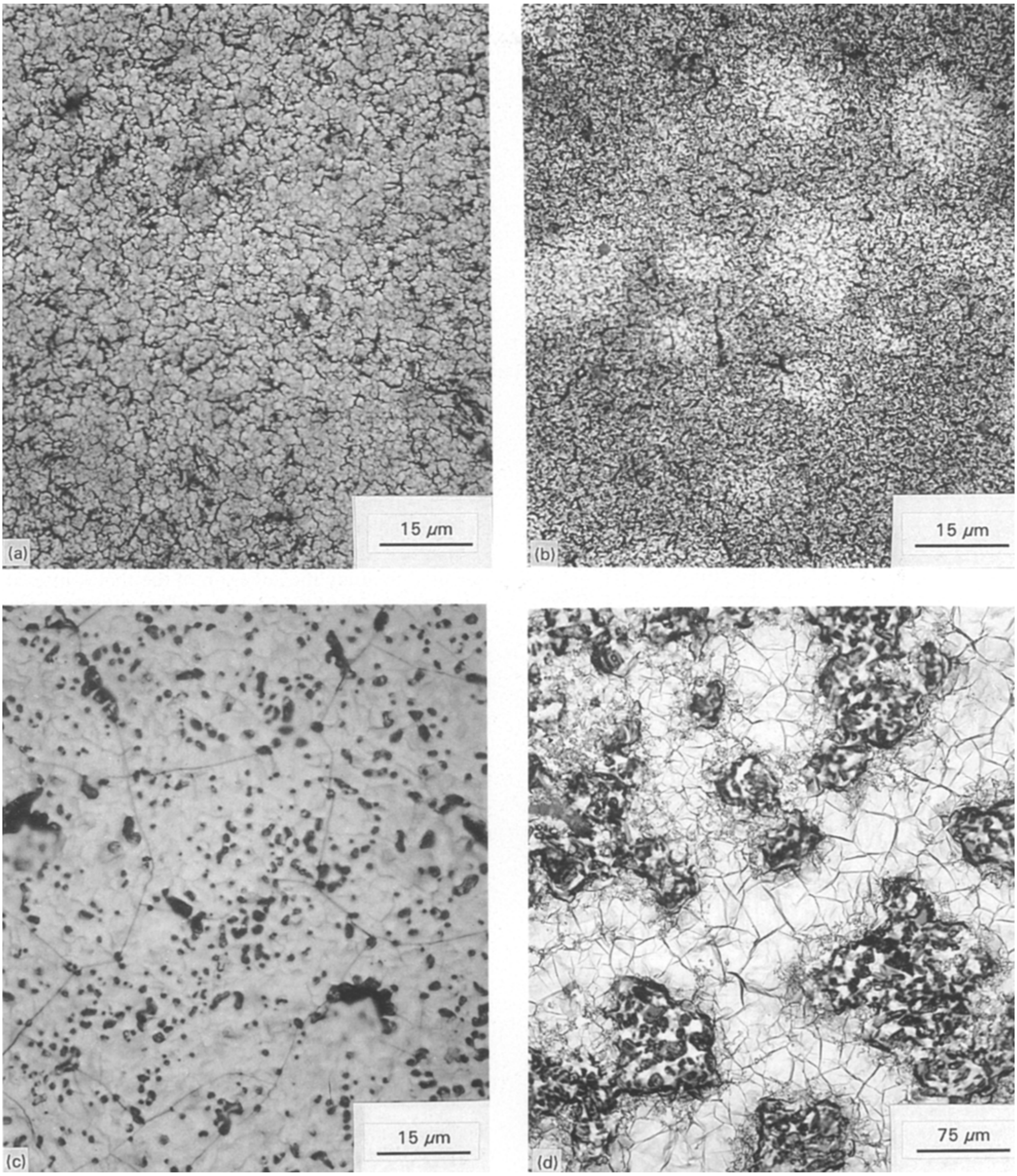

Figure 4 Surface structures of the reaction couples of SiC/Co after annealing at (a) 650 °C, 2 h, (b) 850 °C, 4 h, (c) 1050 °C, 2 h and (d) 1450 °C, 2 h. The thickness of the cobalt film on the SiC substrate was fixed at 2 μm.

temperature, only a CoSi + C region was observed in the reaction zone. It seems that Co_2Si is the first reaction product between Cobalt and SiC under these conditions. The migration rate of silicon in this phase is much higher than that of carbon, and reveals the progress of the reaction up to the full consumption of metallic cobalt. The carbon remains in the neighbourhood of the SiC/Co_2Si interface. On increasing the amount of silicon Co_2Si forms CoSi, which probably dissolved carbon which, during the cooling process is deposited randomly in this phase region.

The cross-section of the sample after reaction at 1250 °C for 2 h was quantitatively analysed by EPMA. The line-scan shows that a periodic maximum of the carbon intensity corresponds to the minimum of the cobalt intensity. The alternating band structure between CoSi and CoSi + C developed at 1250 °C for 0.5 and 2 h could be described as the formation of layers such as CoSi/CoSi + C/CoSi/CoSi + C/ ... /SiC.

An increase in temperature results in an increase in the intensity of the XRD peaks of graphite. While no

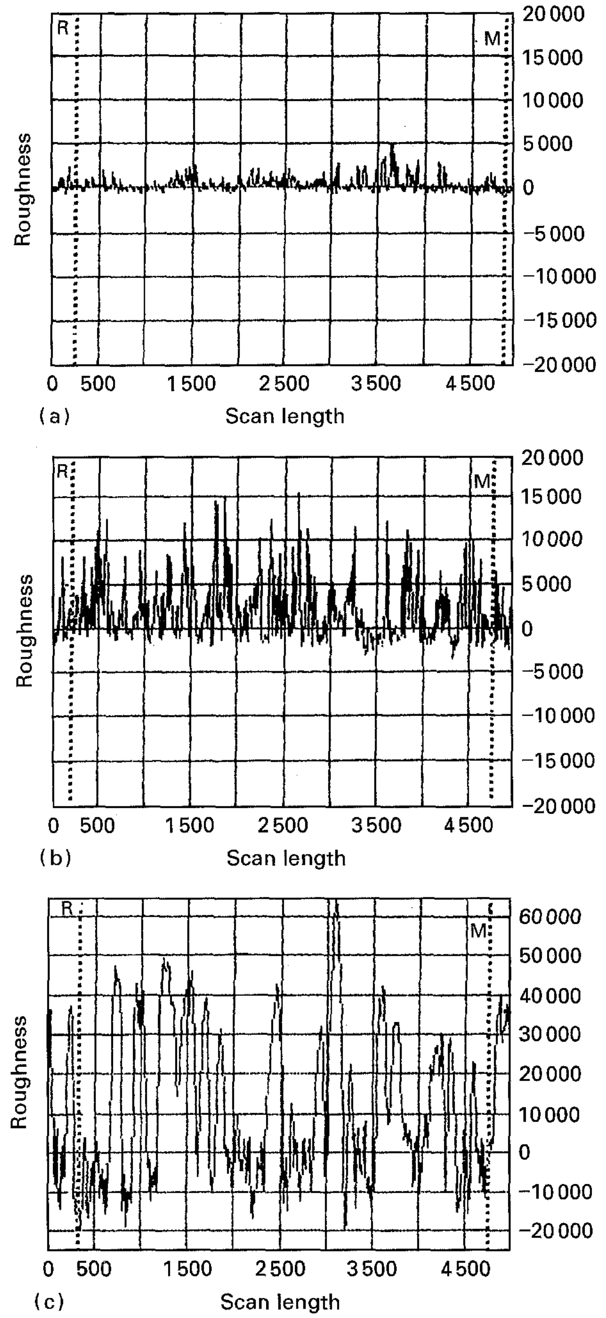

Figure 5 Surface roughness, RA, of annealed cobalt films on SiC at (a) 850 °C, 4 h, (b) 1050 °C, 2 h and (c) 1450 °C, 2 h. RA (a) 0.06, (b) 0.26 and (c) 1.67 μm.

carbide was detected in reacted couples at 1450 °C, CoSi and graphite were detected by XRD. Fig. 10 shows a secondary electron image and X-ray maps with the distribution of the elements carbon, cobalt and silicon in the reaction zone after annealing at 1450 °C for 2 h. The CoSi phase is distributed irregularly at the SiC boundary. Carbon was mainly deposited on the outside of the CoSi phase. At this temperature, a non-periodic structure of carbon precipitates was observed in the CoSi phase. This structure also explains the high X-ray intensity of graphite observed for this sample. The typical phase distribution on the reaction zone from the surface to SiC after annealing at 1450 °C for 2 h can be described as C/CoSi + C/C/SiC.

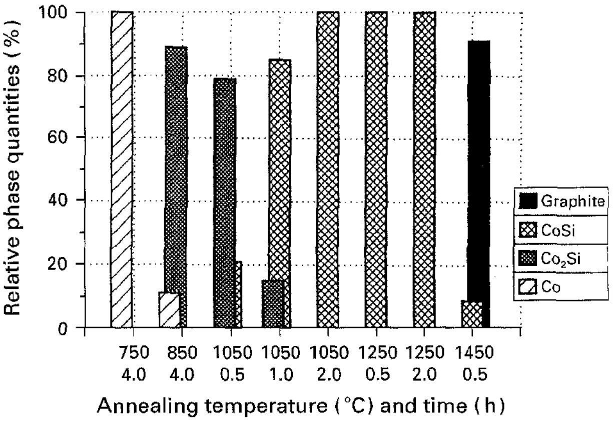

Figure 6 Qualitative analysis of the SiC/Co reaction couples based on relative XRD phase estimation for various annealing conditions.

3.3. Determination of the adhesive strength

The adhesive strength is related to the critical load determined with the scratch test method. A commercially available scratch test apparatus, designed by the Laboratoire Suisse de Recherches Horlogères (LSRH), was used to study the adhesion of the thin sputtered cobalt film on the SiC substrate before and after various anealings. The unit has a diamond stylus in the form of a Rockwell C 120° cone with a spherical tip radius of 0.20 mm. Loads were applied in steps of 100 gf up to a maximum of 20 kgf (1 kgf = 9.8067 N). The load was increased with each traverse until the coating was stripped cleanly from the substrate. The load at which the coating was stripped from the substrate was termed the critical load. Based on the assumption that the coating–substrate interface was subjected to a shear force by the sliding stylus, the critical load, L, gives a value for the adhesive strength, σ_A [13]

$$\sigma_A = KA(HV)/(R^2 - A^2)^{1/2} \tag{1a}$$

and

$$A = [L/\pi(HV)]^2 \tag{1b}$$

which reduces to

$$A = [KL(HV)/\pi R^2]^{1/2} \tag{2}$$

where HV is the substrate hardness if the scratch channel halfwidth, A, is assumed to be much smaller than the stylus radius, R. The constant, L, lies between 0.2 and 1.0 depending on the exact model adopted.

In order to determine the critical load of the reaction couples, an acoustic signal was emitted in the range 0–200 mV. Typical acoustic emission signal curves are illustrated in Fig. 11 for various annealing temperatures (2 h) as a function of stylus load. At low loads the curves are smooth. When coating loss occurs, the signal increases suddenly. The determined critical loads have been compared with microscopy observations. The critical load increased with increasing coating thickness. In this study the coating thickness was fixed at 2 μm. The average values of the critical load of the reaction couples SiC/Co (d_{Co} = 2 μm) are shown in Fig. 12. From the measurements, the average critical loads varied between 6.0

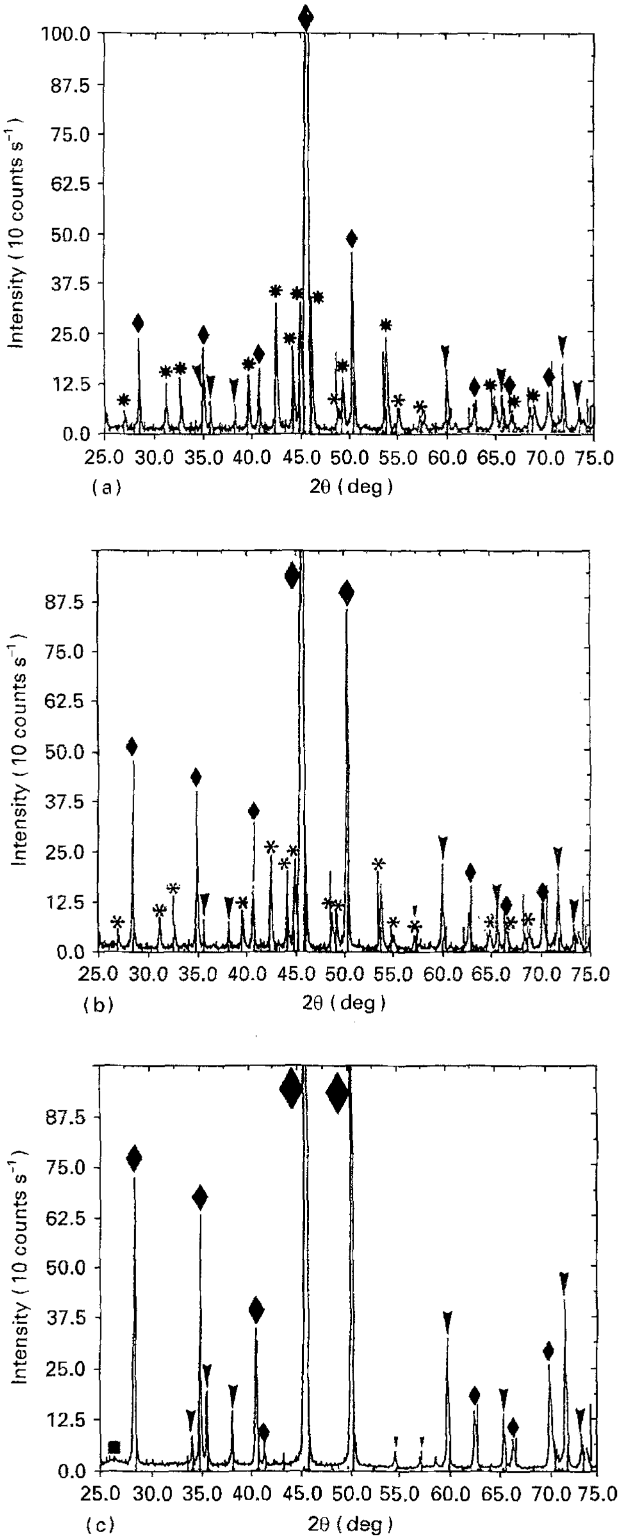

Figure 7 XRD patterns of the reaction products of SiC/Co couples after annealing at 1050 °C for (a) 0.5 h, (b) 1 h and (c) 2 h. (▼) α – SiC, (∗) Co_2Si, (◆) CoSi, (■) C.

TABLE I Relative phase quantities of the silicides from the reaction products after annealing at 1050 °C for various times

	Reaction products	
Annealing time (h)	Co_2Si (%)	CoSi (%)
0.5	78.5	22.7
1.0	25.6	84.4
2.0	0.0	100.0

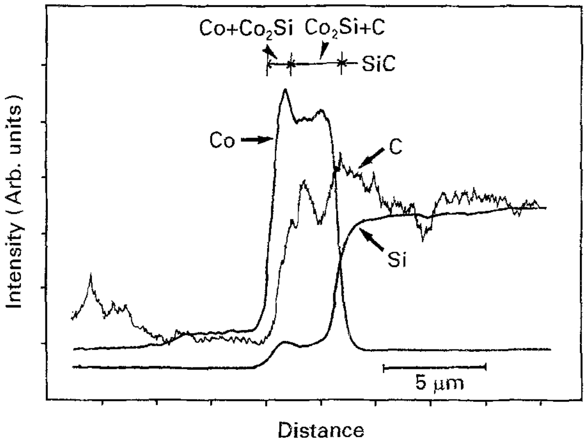

Figure 8 EPMA line scan for cobalt, carbon and silicon over the cross-sectional SiC/Co reaction zone after 4h at 850 °C showing the distinguishable boundary between Co + Co_2Si and Co_2Si + C regions.

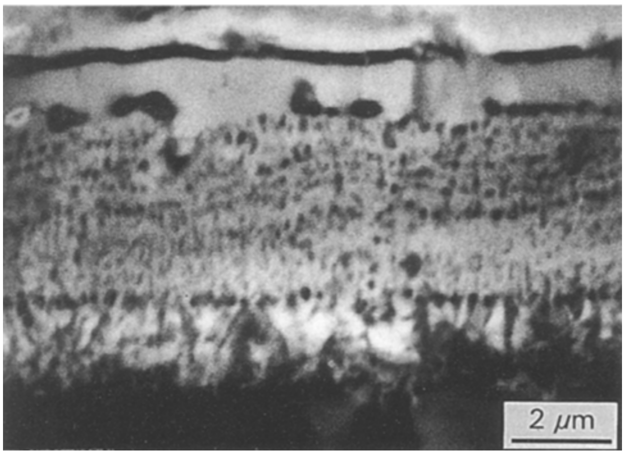

Figure 9 Scanning electron micrograph showing a cross-sectional view of the SiC/Co reaction zone after annealing at 1050 °C for 0.5 h.

and 19 N in temperature ranges between 850 and 1450 °C. Relatively higher values (13–19 N) were observed for couples reacted between 950 and 1050 °C.

4. Discussion

The reaction between cobalt thin film and SiC leads to the formation of cobalt silicides accompanied by carbon precipitates. It is worthwhile discussing the formation of the structure in the reaction zone in terms of the thermodynamics and reaction kinetics. The thermodynamics of the reaction could be described by calculating the Gibb's energy, ΔG_R, for the various reactions within the systems (Table II). In Fig. 13 the calculated values of these reactions are plotted as a function of temperature and compared with the values of the Si/Co system [14]. The result predicts which phases are stable at the thermodynamic equilibrium. Cobalt is known to react with silicon and to form three silicides, Co_2Si, CoSi and $CoSi_2$ (Reactions 5,6 and 7 in Fig. 12), because the ΔG values are highly negative. Less negative values are calculated for the corresponding Reactions 2, 3 and 4 with

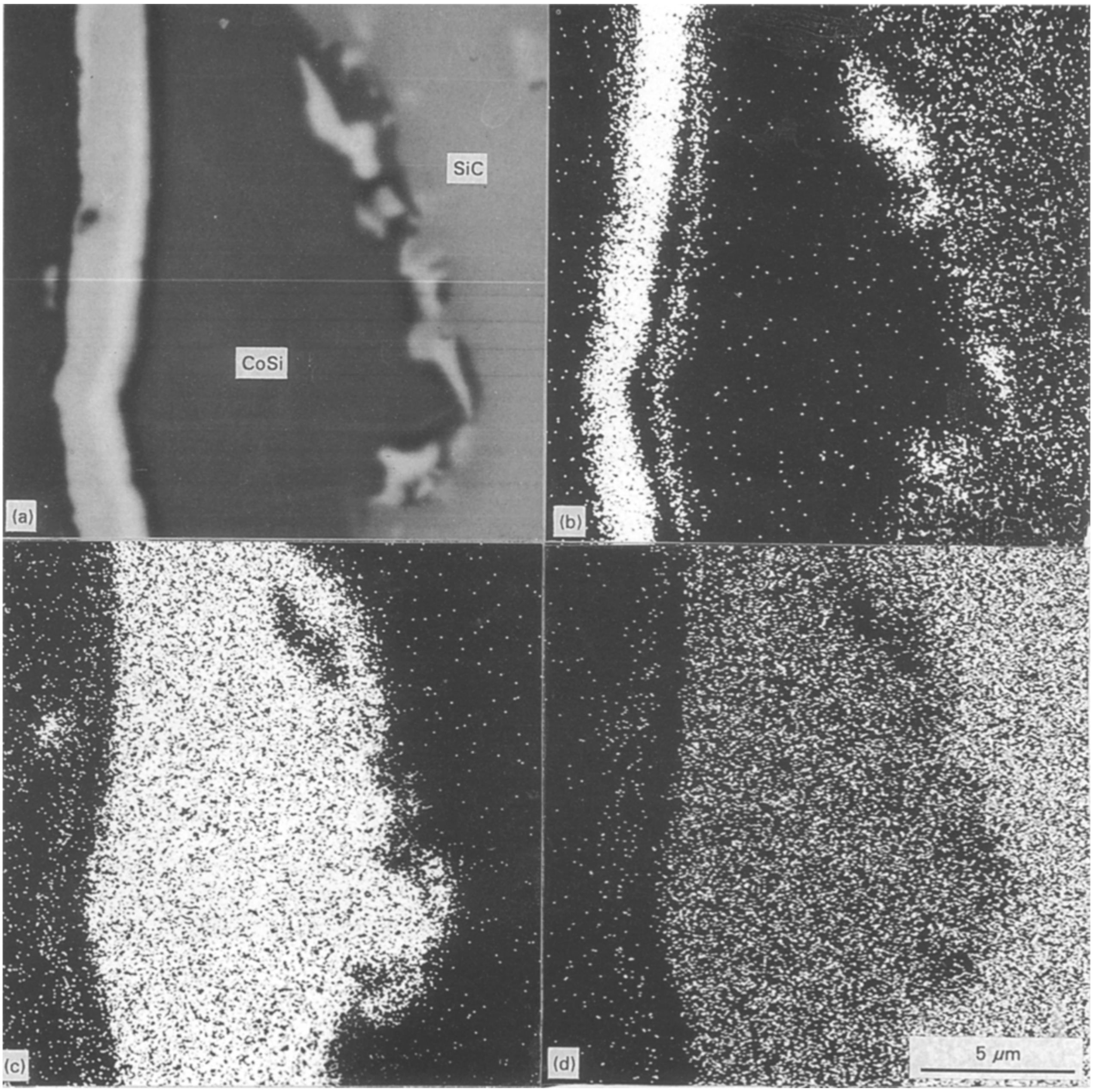

Figure 10 EPMA images of the cross-sectional SiC/Co reaction zone after 2 h at 1450 °C: (a) secondary electron image; (b) carbon X-ray map; (c) cobalt X-ray map; (d) silicon X-ray map.

SiC, because of the energy needed for SiC decomposition. According to the present experimental results, cobalt reacts with SiC and forms various silicides at the SiC interface.

In the case of Reaction 2, where two moles of SiC should be decomposed per reacted cobalt g-atom, ΔG indicates positive values. Therefore, $CoSi_2$ could not be formed in this temperature range. In addition, the formation of the carbide Co_2C (Reaction 1) is thermodynamically impossible under these conditions. Considering the reactions between SiC and cobalt, only the formation of Co_2Si and CoSi shows a negative ΔG value and can be formed by solid state reaction.

At 1050 °C the Co_2Si layer was converted to CoSi and additional carbon precipitates were formed in the CoSi zone. According to reported diffusion data [15–18], cobalt is the dominant diffuser in the Co_2Si phase. It also diffuses through Co_2Si and CoSi and arrives the SiC interface to react with SiC. After the metallic cobalt layer is completely consumed, cobalt migration takes place from the Co_2Si, resulting in the growth of the CoSi layer. It is possible that CoSi grows at the Co_2Si/CoSi and CoSi/SiC interface, resulting in the growth of CoSi with heating time and increasing temperature. Carbon precipitation was only observed in the CoSi phase, because ΔG_R of CoSi is lower than that of the Co_2Si phase and could provide the thermodynamic driving force for carbon precipitation.

5. Conclusion

The reactivity and morphology of thin sputtered cobalt films deposited on SiC were investigated in the temperature range 500–1450 °C. The reaction with the formation of silicides and carbon was first observed

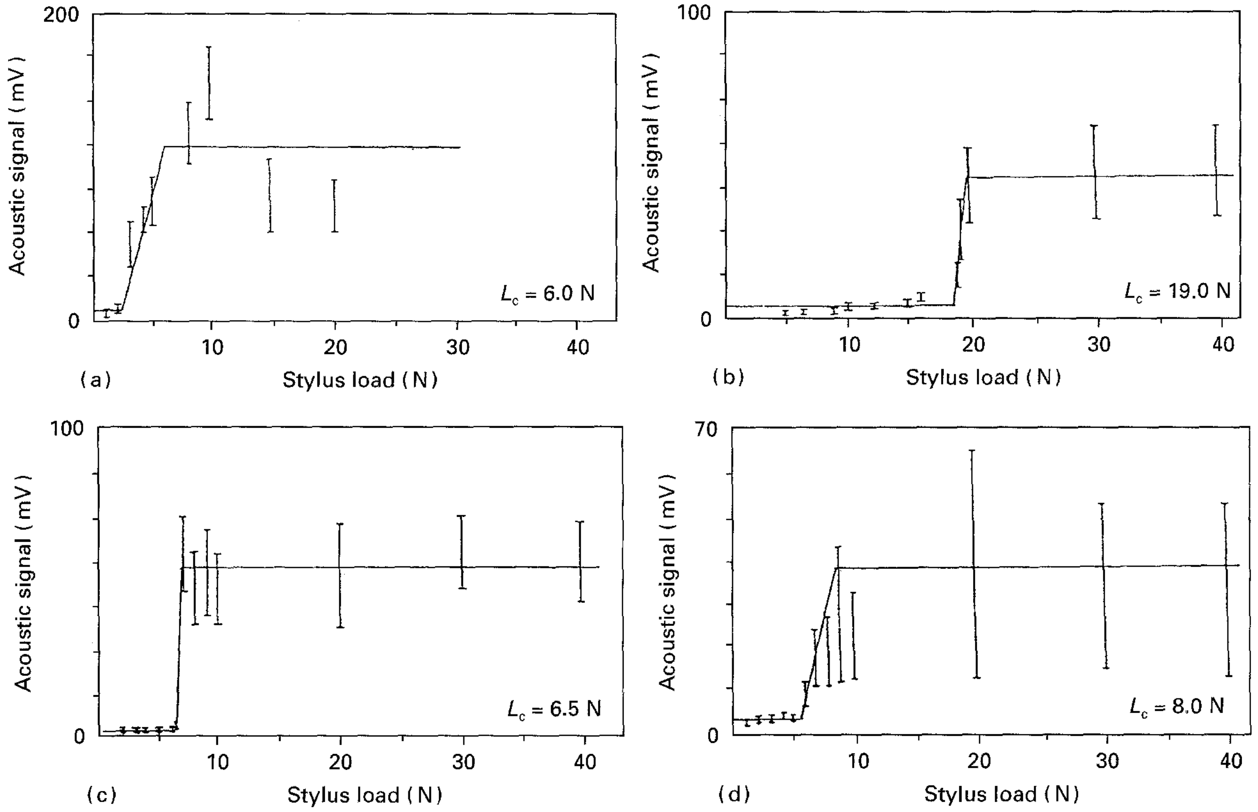

Figure 11 Acoustic signals as a function of stylus load for various reaction couples of SiC/Co after annealings at: (a) 850 °C, 2 h; (b) 1050 °C, 2 h; (c) 1250 °C, 2 h and (d) 1450 °C, 2 h.

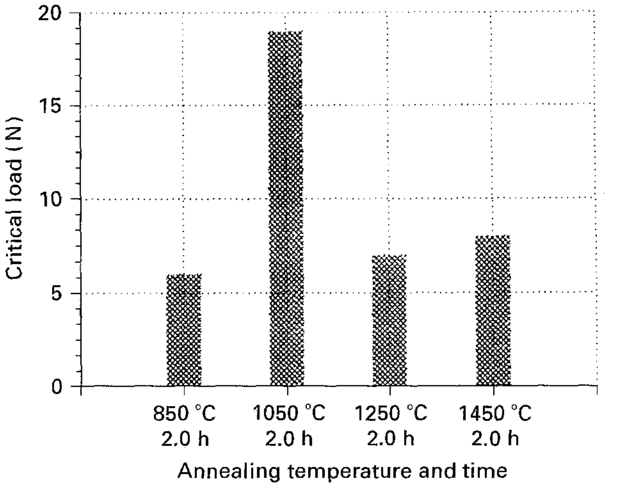

Figure 12 Average critical load of SiC/Co reaction couples determined by the acoustic signal for various heat treatments.

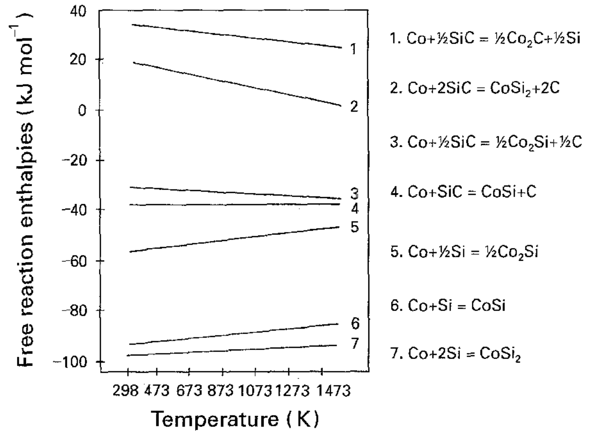

Figure 13 Calculated free reaction enthalpies for various reactions between SiC and cobalt, as well as between silicon and carbon as a function of temperature (based on 1 g-atom Co)

TABLE II Possible reactions and free reaction enthalpies for the SiC/Co system

Possible reactions	Temperature functions of Gibb's energy (kJ mol^{-1})
Co + $\frac{1}{2}$SiC = $\frac{1}{2}$Co$_2$C + $\frac{1}{2}$ Si	ΔG_T = 37.516 + 0.0027 T log T-0.016 T
Co + 2SiC = CoSi$_2$ + 2C	ΔG_T = 18.392 + 0.0108 T log T-0.044 T
Co + $\frac{1}{2}$SiC = $\frac{1}{2}$Co$_2$ Si + $\frac{1}{2}$ C	ΔG_T = -29.061 + 0.0027 T log T-0.0118 T
Co + SiC = CoSi + C	ΔG_T = -36.366 + 0.0054 T log T-0.0176 T

above 850 °C. At 1050 °C, as the reaction proceeded, the initially formed Co$_2$Si layer was converted to CoSi and carbon precipitates were observed within this zone. The thin cobalt film reacted completely with SiC after annealing at 1050 °C for 2 h. The thermodynamically stable CoSi is the only observed silicide in the reaction zone up to 1250 °C. The formation of CoSi layers with carbon precipitates alternated periodically with the carbon-free layers: above 1450 °C, near to the melting point of this silicide (1460 °C), carbon precipitated preferentially on the outer surface of the reaction zone and crystallized as graphite.

The formation of Co$_2$Si + C or CoSi + C according the reaction of SiC with thin sputtered cobalt films was favoured under the experimental conditions, because the Gibb's energy of both reactions is negative. The formation of $CoSi_2$ or the carbide Co_2C is thermodynamically prohibited in this temperature regime, because ΔG of the corresponding reactions has positive values. At 1050 °C, the initially formed Co_2Si layer was converted to CoSi and carbon precipitates were formed in the reaction zone of CoSi.

The adhesive strength was qualitatively compared in terms of the critical load estimated with the scratch test method. According to the measurements, the average critical loads were 6.0–19.0 N in temperature ranges between 850 and 1450 °C. The relatively higher values of 13.0–19.0 N were measured for samples reacted at temperatures between 950 and 1050 °C.

References

1. S. J. DAPKUNAS, *Ceram. Bull.* **67** (1988) 388.
2. K. D. MOERGENTHAR, *Tech. Keram.* **1** (1988) 285.
3. D. L. MCDANELS, T. T. SERAFINI and J. A. DICARLO, *J. Mater. Energy Systems* **8** (1986) 80.
4. R. J. TREW, J. B. YAN and P. M. MOCK, *Proc. IEEE* **79** (1991) 598.
5. H. HOECHST, D. W. NILES, G. W. ZAJAC, T. H. FLEISCH, B. C. JOHNSON and J. M. MEESE, *J. Vac. Sci. Technol.* **B6** (1988) 1320.
6. M. G. NICHOLAS, *Mater. Sci. Res.* **21** (1986) 349.
7. D. J. LARKIN, L. V. INTERRANTE and A. BOSE, *J. Mater. Res.* **5** (1990) 2706.
8. R. E. LOEHMAN, *Ceram. Bull.* **68** (1989) 891.
9. Y. IINO, *J. Mater. Sci.* **26** (1991) 4399.
10. T. C. CHOU and T. G. NIEH, *J. Mater. Res.* **5** (1990) 1985.
11. P. NIKOLOPOULOS, S. AGATHOPOULOS, G. N. ANGELOPOULOS, A. NAOUMIDIS and H. GRÜBMEIER, *J. Mater. Sci.* **27** (1992) 139.
12. E. GYARMATI, W. KESTERNICH and R. FÖRTHMANN, cfi/Ber. DKG 66 (1989) 292.
13. A. J. PERRY, *Thin Solid Films* **78** (1981) 77.
14. O. KUBASCHEWSKI and C. B. ALCOCK, "Metallurgical Thermochemistry" (Pergamon Press, 1983) p. 280.
15. S. S. LAU and J. W. MAYER, *J. Appl. Phys.* **49** (1978) 4005.
16. G. J. VAN GURP, W. F. VAN DER WEG and D. SIGURD, *Ibid.* **49** (1978) 4001.
17. F. M. D'HEURLE and C. S. PETERSSON, *Thin Solid Films* **128** (2985) 283.
18. A. P. BOTHA and R. PRETORIUS, *Ibid.* **93** (1982) 127.

Received 14 June 1994
and accepted 20 January 1995